

Dynamic modelling of nitrous oxide emissions from three Swedish sludge liquor treatment systems

E. Lindblom, M. Arnell, X. Flores-Alsina, F. Stenström, D. J. I. Gustavsson, J. Yang and U. Jeppsson

ABSTRACT

The objective of this paper is to model the dynamics and validate the results of nitrous oxide (N₂O) emissions from three Swedish nitrifying/denitrifying, nitrification and anammox systems treating real anaerobic digester sludge liquor. The Activated Sludge Model No. 1 is extended to describe N₂O production by both heterotrophic and autotrophic denitrification. In addition, mass transfer equations are implemented to characterize the dynamics of N₂O in the water and the gas phases. The biochemical model is simulated and validated for two hydraulic patterns: (1) a sequencing batch reactor; and (2) a moving-bed biofilm reactor. Results show that the calibrated model is partly capable of reproducing the behaviour of N₂O as well as the nitrification/nitrification/denitrification dynamics. However, the results emphasize that additional work is required before N₂O emissions from sludge liquor treatment plants can be generally predicted with high certainty by simulations. Continued efforts should focus on determining the switching conditions for different N₂O formation pathways and, if full-scale data are used, more detailed modelling of the measurement devices might improve the conclusions that can be drawn.

Key words | ASM1, autotrophic denitrification, greenhouse gases, heterotrophic denitrification, modelling, sludge liquor treatment

E. Lindblom

M. Arnell

U. Jeppsson

Division of Industrial Electrical Engineering and Automation (IEA), Department of Biomedical Engineering, Lund University, PO Box 118, SE-221 00 Lund, Sweden

E. Lindblom (corresponding author)

Stockholm Vatten, SE-106 36 Stockholm, Sweden

E-mail: erik.lindblom@stockholm.vatten.se

M. Arnell

SP Technical Research Institute of Sweden, Guterigatan 1D, SE-582 73 Linköping, Sweden

X. Flores-Alsina

Department of Chemical and Biochemical Engineering, Technical University of Denmark, DK-2800 Lyngby, Denmark

F. Stenström

Water and Environmental Engineering, Department of Chemical Engineering, Lund University, PO Box 118, SE-221 00 Lund, Sweden and VA-Ingenjörerna AB, Trädgårdsgatan 12, SE-702 12 Örebro, Sweden

D. J. I. Gustavsson

VA SYD, PO Box 191, SE-201 21 Malmö, Sweden

and

Sweden Water Research, Ideon Science Park, Scheelevägen 15, SE-223 70 Lund, Sweden

J. Yang

Department of Sustainable Development, Environmental Science and Engineering,

Royal Institute of Technology (KTH), Teknikringen 76, SE-100 44, Stockholm, Sweden

and

Swedish Environmental Research Institute (IVL), Valhallavägen 81, SE-100 31, Stockholm, Sweden

INTRODUCTION

Efficient municipal wastewater treatment plant (WWTP) engineering and operation call for plant-wide process

understanding, which can be summarized as mathematical models (Gerbaey *et al.* 2014). Results from recent

doi: 10.2166/wst.2015.534

investigations have shown that some 'optimal' WWTP operational strategies, e.g. operation with intermittent aeration (Yu *et al.* 2010) and/or low dissolved oxygen (DO) set-points (Kampschreur *et al.* 2009) might be 'sub-optimal' in certain respects because of the risk of elevated emissions of the undesired greenhouse gas nitrous oxide (N_2O). This is possibly due to lack of generally applicable knowledge and models that capture all aspects related to N_2O formation and thus an inability of WWTP simulators to predict the emissions with certainty.

Based on new knowledge of the biological mechanisms of N_2O production, recent efforts have been made to capture the production and emission of N_2O and integrate these processes with the traditional activated sludge models (ASM) (Henze *et al.* 2000; Hiatt & Grady 2008; Mampaey *et al.* 2013; Ni *et al.* 2013; Pan *et al.* 2014). The aim is to increase the understanding of the N_2O production mechanisms and eventually to allow for mitigation of the emission, e.g. by developing appropriate control strategies. The paper by Flores-Alsina *et al.* (2014) clearly demonstrates how seemingly good control strategies for WWTPs in terms of improved effluent quality and lower operational costs may actually lead to a dramatic increase in greenhouse gas emissions, thereby partly counteracting the original purpose of the control.

In this study, process models for sequencing batch reactor (SBR) and biofilm systems – including available N_2O production models – for treating sludge liquors from anaerobic digestion of municipal primary, secondary and chemical sludge have been developed, implemented in the software (*Matlab-Simulink*[®]) and evaluated to test if a combination of the above-mentioned biological reaction models can be calibrated and validated using full-scale data.

MATERIAL AND METHODS

Full-scale data sets

The models are calibrated to reproduce the data sets from three Swedish full-scale systems denoted *SBR_N/DN*, *SBR_NO2* and *MBBR_AMX*:

- ***SBR_N/DN***: N_2O measurements performed by Stenström *et al.* (2014), who investigated a nitrification(N)-denitrification(DN) SBR process at Slottshagen WWTP (Norrköping, Sweden);
- ***SBR_NO2***: N_2O measurements performed by Gustavsson & la Cour Jansen (2011), who investigated a *nitritation only* SBR process at Sjölanda WWTP (Malmö, Sweden);

- ***MBBR_AMX***: N_2O measurements performed by Yang *et al.* (2013), who investigated a one-stage nitrification-anammox moving-bed biofilm reactor (MBBR) process at Hammarby-Sjöstad pilot plant (Stockholm, Sweden).

The three case studies involve treatment of real anaerobic digestion sludge liquor and all include measurements of traditional wastewater variables (online and grab samples) and online measurements of N_2O (water and/or gas phase). The reader is referred to the original papers for further details about the experiments.

Mathematical models

Considering the experimental data of the three case studies, a biological process model including heterotrophic ($X_{B,H}$) and ammonia oxidizing bacteria (X_{AOB}) denitrification was hypothesized to be able to describe the measurements. The model was initially based on the ideas summarized in Hiatt & Grady (2008). This model (ASMN) extends the well-recognized ASM1 (Henze *et al.* 2000) with two nitrifying populations: X_{AOB} and nitrite oxidizing bacteria (X_{NOB}). The use of ASMN is partly motivated by the fact that free ammonia (S_{NH_3}) and nitrous acid (S_{HNO_2}) are considered as substrates for X_{AOB} and X_{NOB} , respectively. These components are temperature- and pH-dependent, which is important to consider while modelling sludge liquor treatment processes. Moreover, the sequential four-step heterotrophic denitrification of nitrate (S_{NO_3}) to nitrogen gas (N_2) in the model is via nitrite (S_{NO_2}), nitric oxide (S_{NO}) and nitrous oxide (S_{N_2O}); both S_{NO_2} and S_{NO} are important components to consider for N_2O production by X_{AOB} (Chandran *et al.* 2011). ASMN does not include AOB N_2O production, which, as pointed out by Gustavsson & la Cour Jansen (2011) and Stenström *et al.* (2014) amongst others, potentially is a governing process for N_2O formation in biological sludge liquor treatment systems. To date, N_2O is believed to be produced by AOB through two different pathways (Chandran *et al.* 2011; Ni *et al.* 2014): (1) AOB denitrification; and (2) incomplete oxidation of hydroxylamine, hereby denoted the NH_2OH pathway. In Ni *et al.* (2013), four different models, each including one of the pathways, were compared with data sets from different systems. None of the models could describe all data sets accurately and recently, Ni *et al.* (2014) therefore presented an integrated model in which both pathways are included. Thereby it is suggested that shifts of the dominating pathway, due to different process conditions during nitrification (mainly DO and NO_2^- concentrations), can be

predicted. Unfortunately, the two-pathway model adds significantly to model complexity as electron competition, with several additional model parameters, is included. Since this work considers N₂O production also by heterotrophic denitrification it was, to confine the model complexity, decided to implement a one-pathway model for AOB N₂O production, i.e. the AOB denitrification pathway. Moreover, the model by Ni *et al.* (2014) was not available by the time this project had to decide upon which model to apply. Among the two AOB denitrification models evaluated by Ni *et al.* (2013), the one proposed by Mampaey *et al.* (2013) was selected for implementation because it does not contain additional model components and therefore is relatively easy to integrate with ASMN. In the resulting integrated model, X_{AOB} are also capable of reducing S_{HNO2} to S_{NO} and further into S_{N2O}. The assumed reaction rates for X_{AOB} denitrification ($r_{\text{NO}/\text{N2O},\text{AOB},\text{den}}$ [g N m⁻³ d⁻¹]) are shown in Equations (1) and (2):

$$r_{\text{NO},\text{AOB},\text{den}} = f_{\text{DNT},\text{A}} \cdot \frac{\mu_{\text{AOB}}}{Y_{\text{AOB}}} \cdot \left(\frac{S_{\text{O}}}{K_{\text{O},\text{AOB}} + S_{\text{O}}} \right) \cdot \left(\frac{S_{\text{NH}_3}}{K_{\text{NH}_3,\text{AOB}} + S_{\text{NH}_3}} \right) \cdot \left(\frac{S_{\text{HNO}_2}}{K_{\text{HNO}_2,\text{AOB}} + S_{\text{HNO}_2}} \right) \cdot X_{\text{AOB}} \quad (1)$$

$$r_{\text{N}_2\text{O},\text{AOB},\text{den}} = \frac{\mu_{\text{AOB}}}{Y_{\text{AOB}}} \cdot \left(\frac{S_{\text{O}}}{K_{\text{O},\text{AOB}} + S_{\text{O}}} \right) \cdot \left(\frac{S_{\text{NH}_3}}{K_{\text{NH}_3,\text{AOB}} + S_{\text{NH}_3}} \right) \cdot \left(\frac{S_{\text{NO}}}{K_{\text{NO},\text{AOB}} + S_{\text{NO}}} \right) \cdot X_{\text{AOB}} \quad (2)$$

In the original model, the same half-saturation coefficients $K_{\text{O},\text{AOB}}$ and $K_{\text{NH}_3,\text{AOB}}$ are assumed for X_{AOB} aerobic ammonia oxidation and X_{AOB} denitrification. The parameters $K_{\text{HNO}_2,\text{AOB}}$ and $K_{\text{NO},\text{AOB}}$ are unique for X_{AOB} denitrification. It should be highlighted that, although not included in the presented model, incomplete oxidation of NH₂OH may also play an important role in the N₂O production of the three case studies. Finally, growth and decay processes of anammox active biomass (X_{AMX}) according to Hao *et al.* (2002) were included in the biological process model. X_{AMX} convert S_{NH4} and S_{NO2} to mainly nitrogen gas and also S_{NO3} in the absence of oxygen.

Stripping (mass transfer) equations for the gases were implemented as in Foley *et al.* (2011). In the three case studies, the monitored DO concentration is used as the input to a controller that adjusts the $k_L a_{\text{O}_2}$ of the modelled

systems. The applied diffusivities of N₂O and O₂ are 1.77 · 10⁻⁹ m²/s and 2.12 · 10⁻⁹ m²/s, respectively, yielding $k_L a_{\text{N}_2\text{O}} = 0.91 k_L a_{\text{O}_2}$. The simulated flux of N₂O in the off-gas ($F_{\text{N}_2\text{O}}$ [kg N d⁻¹]), which is used to validate the model behaviour with the measured emissions, is then given by $F_{\text{N}_2\text{O}} = k_L a_{\text{N}_2\text{O}} \cdot S_{\text{N}_2\text{O}} \cdot V_{\text{AER}}$, with V_{AER} [m³] denoting the aerated water volume. The simulated $k_L a_{\text{O}_2}$ values are within the range of 300 to 600 d⁻¹. Thus, the half-life of possibly accumulated S_{N2O} during stripping is only a few minutes. Any long-term dynamic variation of N₂O emissions is therefore, according to the model, due to variations of the biological reaction rates. However, the stripping/flux equation might represent an overly simplified version of reality. For example, the retention time of the bubbles in the reactor, the measurement devices and stripping during non-aerated conditions have not been taken into account.

The reactive settler model developed within the benchmark simulation model (BSM) framework (Flores-Alsina *et al.* 2012) was expanded with variable layer heights (e.g. during filling) and layer mixing (e.g. during aeration) to describe the SBR behaviour of the SBR_N/DN and SBR_NO2 systems.

The biofilm model, used to model the MBBR anammox system (MBBR_AMX), was inspired by the implementation in the commercial software platform WEST 3.7.3 (DHI 2011). According to this model, the bulk water volume is separated from the biofilm, which, in turn, is divided into 10 layers. Soluble components are transported by diffusion between the biofilm layers and bulk, proportionally to the concentration gradients. Particulate material attaches to the outermost layer of the biofilm and detachment occurs from all layers as the biofilm thickness exceeds a user defined maximum value.

RESULTS AND DISCUSSION

In this section, the results of the three case studies are shown and discussed. A summary of applied parameter values is given in Table 1.

Nitrification/denitrification SBR, case SBR_N/DN

Recorded DO and pH values (Figures 1(a) and 1(d)) as well as flow rate data were directly used as model inputs. The process temperature was constant (30.3 °C).

During the measurement period of 16 hours used for model calibration the NH₄⁺-N load to the SBR plant was 180 kg N d⁻¹. The SBR_N/DN cycle of 8 hours starts with 3.5 hours of anoxic denitrification including 2 hours of

Table 1 | Calibrated model parameter values for the three case studies

	K_{S5} [g COD·m ⁻³]	$K_{S,EtOH,5}$ [g COD·m ⁻³]	K_{N2O} [g N·m ⁻³]	b_{AOB} [d ⁻¹]	μ_{AOB} [d ⁻¹]	$f_{DNT,A}$ [-]
Reference	40 ^a		0.0007–0.001 ^b	0.13 ^c	2.13 ^d ; 2.05 ^c	0.028 ^d
SBR_N/DN	100	1	0.001	0.23	2.00	0.120
SBR_NO2	40	–	–	0.23	0.85	0.075
MBBR_AMX	40	–	–	0.08	1.41	–
	Y_{AOB} [g COD·(g N) ⁻¹]	$K_{O,AOB}$ [g O ₂ ·m ⁻³]	$K_{NH3,AOB}$ [g N·m ⁻³]	$K_{NH3,AOB,DN}$ [g N·m ⁻³]	$K_{HNO2,AOB}$ [g N·m ⁻³]	$K_{NO,AOB}$ [g N·m ⁻³]
Reference	0.18 ^a ; 0.15 ^{b,c}	0.6 ^a ; 0.5 ^d	0.0075 ^a ; 1.0 ^d	1.0 ^d	0.002 ^d	1.0 ^d
SBR_N/DN	0.18	1.0	0.053	0.368	0.003	0.06
SBR_NO2	0.18	1.0	0.140	1.000	0.001	0.06
MBBR_AMX	0.18	1.0	0.053	–	–	–

Values from original publications given in italics:

^aHlatt & Grady (2008).

^bZhou et al. (2008).

^cHao et al. (2002) at T = 30 °C.

^dMaupaey et al. (2013) at T = 35 °C.

filling. Initially, the accumulation rate of S_{N2O} is almost equal to the denitrification rate of S_{NO3} indicating that the final step of heterotrophic denitrification is inhibited (Figures 1(c) and 1(g)). At $t = 1.5$ h ethanol is dosed to the process and S_{N2O} in the water phase is immediately reduced. To model these observations with ASMN the heterotrophic N_2O denitrification process without ethanol must be almost completely inhibited. The original ASMN inhibition term for S_{NO} was replaced by S_{NO2} inhibition (Zhou et al. 2008) since no information of S_{NO} concentrations was available. Despite several attempts this drastic shift, between complete and no inhibition because of a low availability of readily biodegradable substrate (S_S), could not be captured by the original ASMN model and motivated the extension with an additional model component representing ethanol, $S_{S,EtOH,5}$ [g COD·m⁻³]. This state variable was assumed to affect the process in the same way as S_S , with the exception that the half-saturation coefficient ($K_{S,EtOH,5}$) for the last step of denitrification, heterotrophic growth with $S_{S,EtOH,5}$ as substrate and N_2O as electron acceptor, is set to a low value (1 g COD·m⁻³). For the same process, but with S_S from the influent sludge liquor as substrate, the half-saturation coefficient (K_{S5}) was given a high value (100 g COD·m⁻³). Although there might be a physical explanation for the varying values of the half-saturation coefficients, they should in this case be considered as lumped values to model the inhibition without external carbon. However, according to the simulation results, S_{N2O} starts to accumulate again as ethanol is consumed, a phenomenon that was not measured and indicates that separated growth on internal and added substrates is not necessarily the actual process governing the S_{N2O} formation. Pan et al. (2014) recently published a new model for the denitrification process that, in comparison with ASMN, better describes electron competition and the dynamics of denitrification intermediates in a number of experiments. Adopting the concepts of this model might be a way to fully describe the observed heterotrophic denitrification process of the SBR_N/DN case.

Ammonia oxidation starts instantly when aeration is initiated at $t = 3.5$ h (Figures 1(a) and 1(b)). The associated N_2O emissions are shown in Figure 1(f). A sharp peak in the simulated emission is seen at the start of the aeration due to stripping of the partially faulty prediction of anoxic N_2O accumulation (Figure 1(g) between $t = 3.0$ – 3.5 h). The maximum measured N_2O emission is reached after 1 hour of aeration with absence of measured accumulated S_{N2O} from the preceding anoxic phase. Thus, the emission is mainly due to N_2O production during aerobic conditions and according to the implemented model to AOB

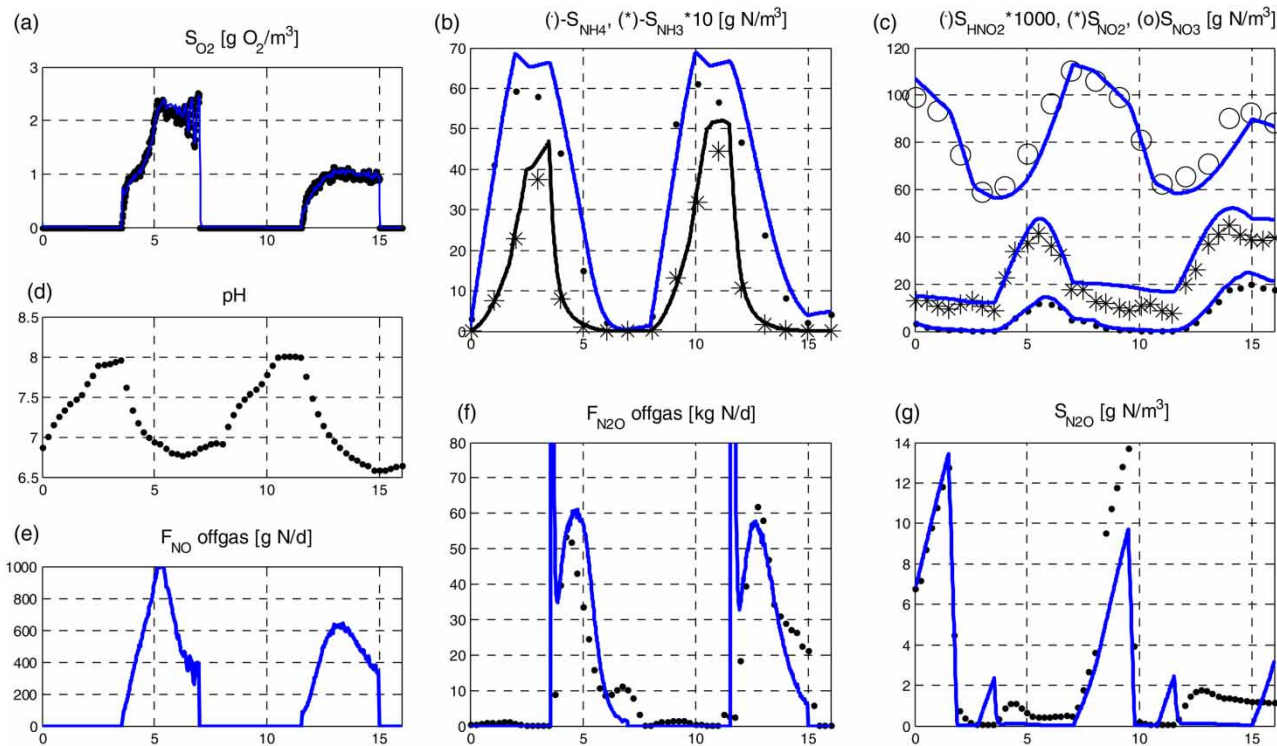


Figure 1 | Measured (markers) and simulated (solid lines) concentrations and mass flows for the nitrification/ denitrification SBR process (*SBR_N/DN*). Measurements of NO (e) were not available. The x-axes show time in hours.

denitrification. The X_{AOB} affinity coefficient for S_{HNO_2} appears relatively low since S_{HNO_2} peaks after 2.5 hours of aeration (Figure 1(c)). As will be shown in the next case study as well, the studied emission seems to be correlated with S_{NH_3} and in the model this has been accounted for by choosing a separate half-saturation coefficient for S_{NH_3} during AOB denitrification, $K_{NH_3,AOB,DN}$ [$g\ N \cdot m^{-3}$]. The used value is seven times higher compared with the value of $K_{NH_3,AOB}$ ($0.053\ g\ N \cdot m^{-3}$) for aerobic ammonia oxidation, see Table 1. It must be stated that incomplete NH_2OH oxidation might also contribute to the emission but according to results in Ni et al. (2014), the moderate concentrations of NO_2^- ($15\text{--}40\ mg\ N\ L^{-1}$) and DO ($1\text{--}2\ mg\ O_2\ L^{-1}$) supports the assumption that AOB denitrification is the dominating pathway in this case.

Nitrification only SBR, case *SBR_NO2*

During the measurement period of 24 hours used for model calibration the NH_4^+-N load to the SBR plant was $710\ kg\ N\ d^{-1}$. The temperature in the SBR process was similar to *SBR_N/DN*, $31.7^\circ C$. An important difference is, however, that in *SBR_NO2* the pH was controlled at 6.8. The *SBR_NO2* cycle of 6 hours starts with aeration and

filling. S_{NH_4} increases until filling stops after 1.5 hours (Figure 2(b)). During the subsequent aerobic batch mode phases, the nitrification process proceeds until aeration is switched off. A fixed constant airflow is applied during each cycle but the total length of the aerated phases is varied. This also means that the time periods for the anoxic settling phases that make up the end of each cycle vary.

The SBR process had been operated for nitrification only during several months prior to this measurement campaign and the sludge was therefore enriched with X_{AOB} . The DO data (Figure 2(a)) indicate that the oxygen demand of the sludge decreases when S_{NH_4} decreases below $50\ g\ N\ m^{-3}$, which was modelled by a half-saturation coefficient ($K_{NH_3,AOB}$) value of $0.14\ g\ N\ m^{-3}$, corresponding to $24\ g\ NH_4-N\ L^{-1}$.

The sharp simulated peaks at the beginning of each phase (not reflected in the measurement data) are due to stripping of accumulated S_{N_2O} during anoxic conditions. Consequently, as stripping according to the model occurs fast, the decrease in N_2O production throughout the aeration phase must be explained by aerobic biological N_2O production.

The N_2O emissions reach $30\text{--}75\ kg\ N\ d^{-1}$ and decrease to $10\text{--}15\ kg\ N\ d^{-1}$ at the end of the aerobic phases (Figure 2(e)). In the most extreme cycle (#4, $t = 18\text{--}24\ h$), the emission at the end of the aerated phase is only 20% of the maximum

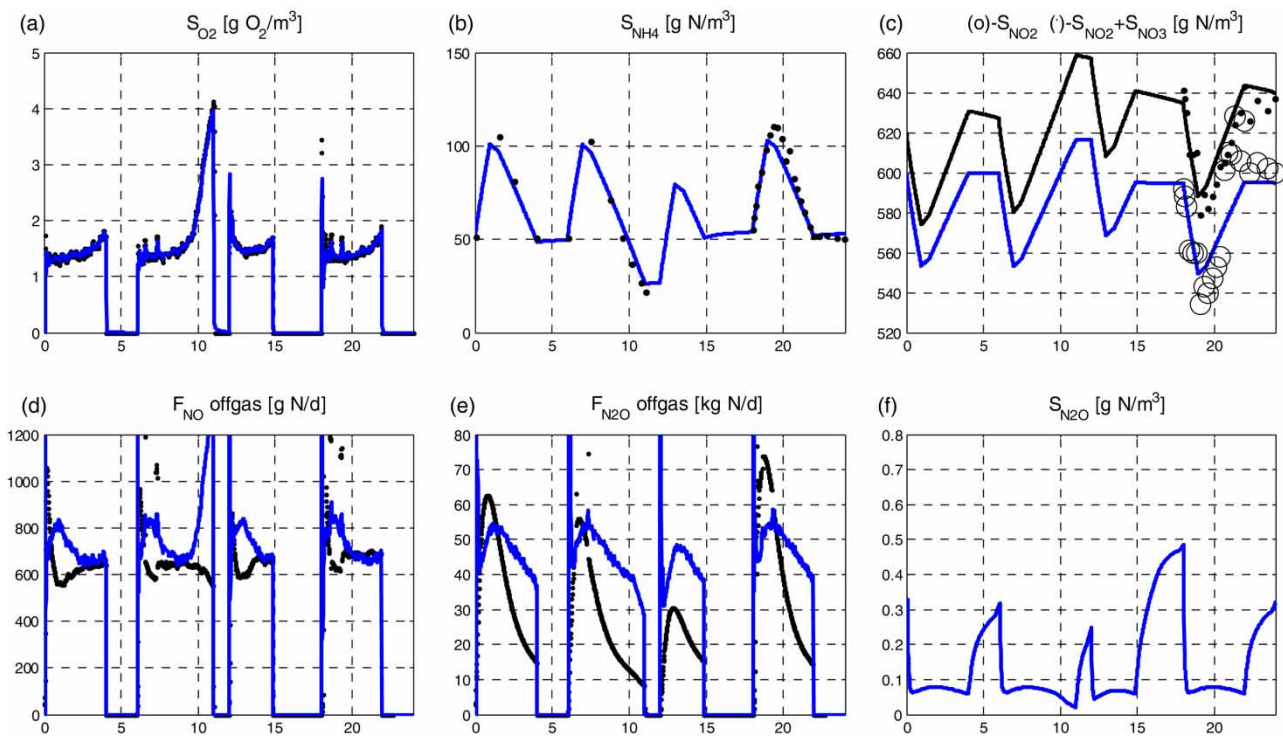


Figure 2 | Measured (markers) and simulated (solid lines) concentrations and mass flows for the nitritation only SBR process (*SBR_NO2*). Measurements of dissolved N_2O (f) were not available. The x-axes show time in hours.

emission during that same phase. Considering Equation (1), S_{NO_2} in the process varies around 500–600 $g N m^{-3}$ during the nitritation phase (Figure 2(c)). This variation corresponds to 0.15–0.18 $g HNO_2 \cdot N \cdot m^{-3}$ with the pH being controlled at = 6.8 and a temperature of 31.7 °C. Since the concentrations are always high they are believed not to represent any major cause for the varying N_2O emissions. S_O actually increases throughout the aeration phase, a phenomenon that according to the model could increase the N_2O production (in contrast to the observations).

Opposite to the *SBR_N/DN* case this study includes measurements of NO offgas concentrations, which were relatively stable. This is reflected by the almost constant calculated NO emissions shown in Figure 2(d). Considering Equation (2), S_{NO} does therefore not explain the dynamic N_2O emissions.

The attempt to fit the AOB denitrification model (Equations (1) and (2)) to the measurement data is not successful and requires the inclusion of – as was also done for *SBR_N/DN* – a unique S_{NH_3} half-saturation coefficient for AOB denitrification ($K_{NH_3,AOB, DN}$). By choosing a high value (1.0 $g N m^{-3}$) the S_{NH_3} dependency changes towards a linear relation and part of the dynamics can be modelled.

In the original paper describing the experimental data (Gustavsson & la Cour Jansen 2011), a linear relation between the length of the anoxic phase and emitted mass of N_2O was proposed. The implemented model can be adjusted to explain this phenomenon as seen in the varying peak S_{N_2O} concentrations before aeration (Figure 2(f)). However, as already noted, the sharp peaks in the simulated emissions due to stripping were not experimentally supported.

The overall conclusion based on the reasoning above, and several attempts to simulate the model with various parameter sets, is that the ASMN/Mampaey model may not be feasible for explaining the complete dynamics of nitrous oxide emissions from *SBR_NO2*.

It has been shown by laboratory experiments (Law et al. 2013) and modelling (Ni et al. 2014) that the high nitrite concentrations (500–600 $g N m^{-3}$) in combination with moderate DO concentrations (1.2–2.0 $mg O_2 L^{-1}$ of case *SBR_NO2*) would imply that the contribution of the NH_2OH pathway to the total N_2O emission is substantial. As was shown above (Figure 2) it is difficult to calibrate the Mampaey AOB denitrification model to the data without applying a very high value of the $K_{NH_3,AOB, DN}$ parameter (1.0 $mg NH_3-N/L$ or 175 $mg NH_4-N/L$). The NH_2OH pathway model presented by Law et al. (2012) could potentially

describe the data better. In that model it is assumed that the intermediates NH_2OH and NOH can accumulate if the AOB NH_3 oxidation process rate is high (e.g. at high DO and high S_{NH_3}). N_2O production is then modelled following first-order kinetics as chemical decomposition of NOH . Thus if the accumulation proceeds so that the concentration of NOH is linearly proportional to S_{NH_3} the NH_2OH pathway model could probably better describe the observations of case *SBR_NO2*.

MBBR anammox, case (*MBBR_AMX*)

The influent sludge liquor originated from the full-scale anaerobic digestion process at Bromma WWTP in Stockholm, Sweden. During the measurement period of 24 hours used for model calibration the ammonia load to the pilot-scale reactor was 70 g N d^{-1} or $1.7 \text{ g N} \cdot (\text{m}^2 \text{ d})^{-1}$. This load corresponds to, compared to other periods, a low load and the amount of biomass in the system should therefore not have limited the total N removal efficiency (88%). The pH and temperature were relatively constant at 7.1 and 25°C , respectively.

The simulated amounts of biomass in the bulk and biofilm are shown in Figure 3(a). X_{AMX} dominates and is

present throughout the entire biofilm. The process is intermittently aerated 45 out of 60 minutes (Figure 3(d)) and X_{AMX} therefore has the possibility to also grow in the outer layers. X_{AOB} and a small amount of X_{NOB} are also present in the outer layers. Note that a significant amount of biomass is found in the bulk water volume (shown as dots in Figure 3(a)). In the model, and according to experimental observations, there is heterotrophic activity in the system as well due to decay and a small amount of biodegradable organic matter present in the influent.

Simulation results show that, compared to the previous case studies, the relatively low N_2O emissions of 0.5% during the studied period can be explained by heterotrophic denitrification. In the demonstrated simulations (Figure 3), the ASMN default parameters for $X_{\text{B,H}}$ were used. Approximately 3% of the influent S_{NH_4} is converted via nitrification and heterotrophic denitrification and 20% out of this amount is accumulated as $S_{\text{N}_2\text{O}}$, probably because of low S_{S} concentrations from hydrolysis of particulates in the biofilm. The resulting emissions of N_2O are similar to the measurements and therefore, to simplify, the AOB denitrification process equations of the model was deactivated in this case. It should, however, be noticed that higher emission rates of N_2O were measured during other periods of the

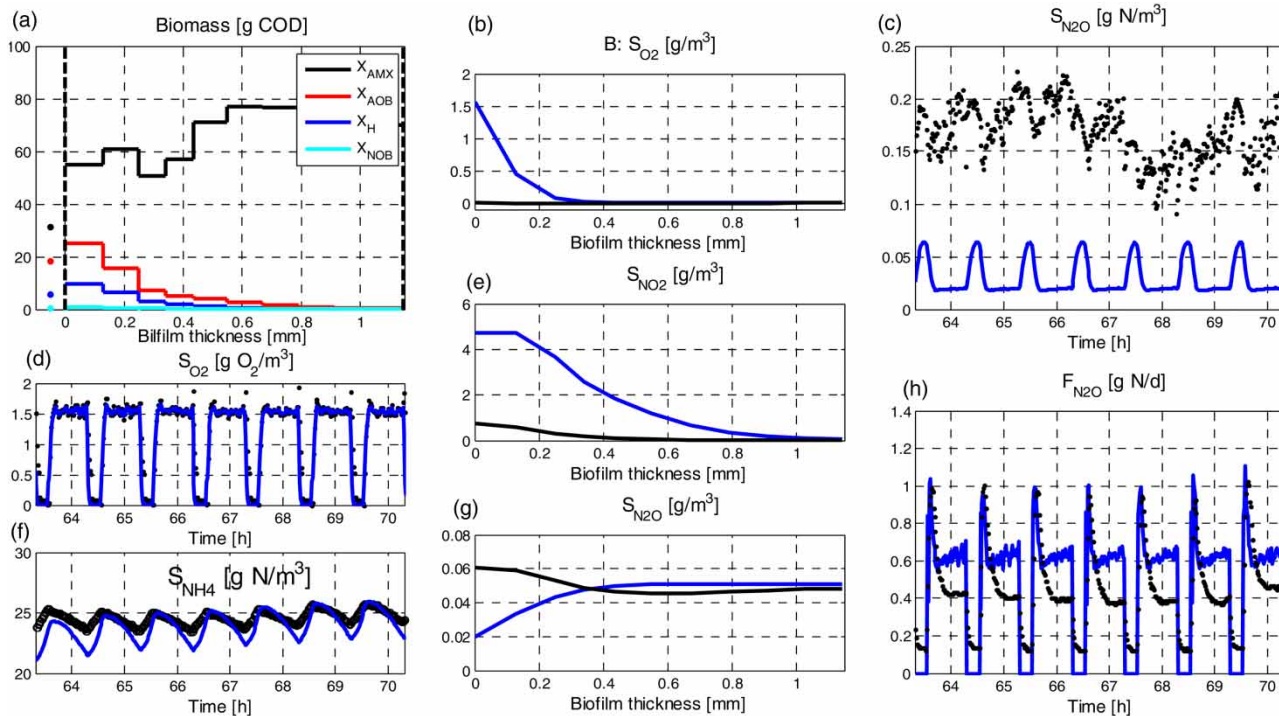


Figure 3 | Scenario *MBBR_AMX*. (a): Simulated amounts of active biomass in each of the 10 biofilm layers (lines) and bulk (dots). In total, the biofilm (40 m^2) contains 1,200 g TS (solids). (b), (e), (g): Simulated concentration profiles during the end of aerobic (blue line) and anoxic (black line) conditions. (c), (d), (f), (h): Measured (markers) and simulated (solid lines) concentrations and mass flows. (c), (d) and (f) show bulk concentrations. Please refer to the online version of this paper to see this figure in colour.

measurement campaign with higher nitrogen loads and different DO operational settings, which might indicate AOB denitrification and/or incomplete NH_2OH oxidation. The reader is referred to Yang *et al.* (2013) for further information.

Figure 3(f) shows the simulated and measured bulk S_{NH_4} concentrations. S_{NO_3} varies between 60 and 65 g N m^{-3} and both S_{NH_4} and S_{NO_3} fully penetrate the modelled biofilm. Figures 3(b), 3(e) and 3(g) show simulated concentration profiles from the bulk water through the biofilm layers on two occasions. The black line shows the profile after 15 minutes of anoxic conditions in the bulk while the grey (blue) line shows concentrations after 45 minutes of aeration. From these results it can be seen that S_{NO_2} (Figure 3(e)) is produced in the outer layer during aerobic conditions and penetrates almost the entire biofilm. When aeration is turned off, S_{NO_2} is consumed by X_{AMX} and $X_{\text{B,H}}$. During anoxic conditions, $S_{\text{N}_2\text{O}}$ diffuses into the biofilm where it is converted by heterotrophic denitrifiers. As aeration is turned on $S_{\text{N}_2\text{O}}$ in the bulk volume decreases due to stripping and the diffusion changes direction so that $S_{\text{N}_2\text{O}}$ moves from the biofilm to the bulk.

The simulated N_2O emissions are shown in Figure 3(h). Although much lower, emissions were also measured during non-aerated phases, a phenomenon that was not included in the model. The simulated and measured dissolved N_2O concentrations are shown as time-series in Figure 3(c). $S_{\text{N}_2\text{O}}$ accumulates during anoxic conditions, which is also seen as peaks in the N_2O emission as aeration is turned on. The measurement data do not show a clear pattern but occasionally it can be seen that $S_{\text{N}_2\text{O}}$ increases during anoxic conditions. The simulated $S_{\text{N}_2\text{O}}$ concentrations are generally lower than the measured ones. Based on the implemented model it is difficult to calibrate this effect because $F_{\text{N}_2\text{O}}$ (which is quite well predicted) is proportional to $S_{\text{N}_2\text{O}}$ and $k_{\text{LA}_{\text{N}_2\text{O}}}$. Thus, if the measurements are correct, either the stripping/flux model (including the diffusion coefficients) or the estimated $k_{\text{LA}_{\text{O}_2}}$ need to be modified.

Applied parameter values

In Table 1, a summary of the parameter values for $X_{\text{B,H}}$ and X_{AOB} are shown. The table includes the values that differ from the original publications and show the major differences between the three case studies. Significant inhibition of heterotrophic denitrification was observed in *SBR_N/DN* only motivating the parameter values K_{S_5} , $K_{\text{S}_{\text{EtOH},5}}$ and $K_{\text{I}_{5,\text{HNO}_2}}$. The high value of $K_{\text{NH}_3,\text{AOB}}$ in *SBR_NO2* is probably due to the nitrification only operation with rather

high NH_3 concentrations. A plausible explanation for the lower value of μ_{AOB} in *SBR_NO2* compared to *SBR_N/DN* is inhibition due to the high HNO_2 concentrations. High concentrations of NO_2^- have been shown to have an inhibitory effect on AOB N_2O production as well (Law *et al.* 2013). However, since there are no available data with low NO_2 concentrations in the *SBR_NO2* case this cannot be validated and the potential inhibition effect is therefore lumped into the calibrated value of the $f_{\text{DNT,A}}$ parameter. AOB denitrification was not simulated in *MBBR_AMX* and therefore values of $f_{\text{DNT,A}}$, $K_{\text{NH}_3,\text{AOB,DN}}$, $K_{\text{HNO}_2,\text{AOB}}$ and $K_{\text{NO},\text{AOB}}$ are not given for this case.

CONCLUSIONS

The implemented biological process model, together with physical models for the *SBR*- and *MBBR*-processes, can partly describe the N_2O emission data from the three case studies.

The AOB denitrification model, which was adopted from Mampaey *et al.* (2013), could adequately describe the behaviour of the nitrifying/denitrifying *SBR* (*SBR_N/DN*). For the *nitrification only* *SBR* system (*SBR_NO2*) a high correlation to the ammonia concentration had to be assumed and may indicate that the implemented model is not able to fully describe the dynamics of the real system. It is possible that N_2O production by incomplete oxidation of NH_2OH , which was not included in the model, is dominating in this case.

The four-step denitrification model, which was adopted from Hiatt & Grady (2008), could be used to model accumulation of dissolved N_2O during anoxic conditions in the nitrifying/denitrifying *SBR* (*SBR_N/DN*). To model the drastically decreased N_2O emission caused by addition of ethanol, an additional COD state variable had to be added.

The stripping/flux equation in the implemented model may be overly simplified. It results in sharp N_2O gas emission peaks that are not observed experimentally. For simulation of full-scale N_2O emission data in general, the retention time of the gas including the measurement devices would probably improve the conclusions that can be drawn regarding N_2O formation pathways.

The N_2O emissions from the studied *MBBR* anammox process (*MBBR_AMX*) data were satisfactorily simulated by assuming heterotrophic denitrification only. Results from other studies, indicate that AOB N_2O production may occur as well.

ACKNOWLEDGEMENTS

Dr Lindblom, Mr Arnell and Ms Yang acknowledge the financial support obtained through the Swedish Research Council Formas (contract no. 211-2010-141 and 211-2010-148), the Swedish Water & Wastewater Association (contracts no. 10-106, 10-107 and 11-106) and the J. Gust. Richert Memorial Fund (contract no. PIAH/11:58). Dr Flores-Alsina gratefully acknowledges the financial support provided by the People Program (Marie Curie Actions) of the European Union's Seventh Framework Programme FP7/2007–2013 under REA agreement 329349. Results based on this paper were presented at the IWA World Water Congress in Lisbon, Portugal, 21–26 September 2014.

REFERENCES

- Chandran, K., Stein, L., Klotz, M. & van Loosdrecht, M. 2011 Nitrous oxide production by lithotrophic ammonia-oxidizing bacteria and implications for engineered nitrogen-removal systems. *Biochem. Soc. Trans.* **39**, 1832–1837.
- DHI 2011 *WEST: Modelling Wastewater Treatment Plants – User Guide*. DHI, Hørsholm, Denmark.
- Flores-Alsina, X., Germaey, K. V. & Jeppsson, U. 2012 Benchmarking biological nutrient removal in wastewater treatment plants: influence of mathematical model assumptions. *Water Sci. Technol.* **65** (8), 1496–1505.
- Flores-Alsina, X., Arnell, M., Amerlinck, Y., Corominas, L., Germaey, K. V., Guo, L., Lindblom, E., Nopens, I., Porro, J., Shaw, A., Snip, L., Vanrolleghem, P. A. & Jeppsson, U. 2014 Balancing effluent quality, economic cost and greenhouse gas emissions during the evaluation of (plant-wide) control/operational strategies in WWTPs. *Sci. Total. Environ.* **466–467**, 616–624.
- Foley, J., Yuan, Z., Keller, J., Senante, E., Chandran, K., Willis, J., van Loosdrecht, M. C. M. & van Voorthuizen, E. 2011 *N₂O and CH₄ Emission from Wastewater Collection and Treatment Systems*. Technical report, Global Water Research Coalition, London, UK.
- Germaey, K. V., Jeppsson, U., Vanrolleghem, P. A. & Copp, J. B. 2014 *Benchmarking of Control Strategies for Wastewater Treatment Plants*. Scientific and Technical Report No. 23, IWA Publishing, London, UK.
- Gustavsson, D. J. I. & la Cour Jansen, J. 2011 Dynamics of nitrogen oxides emission from a full-scale sludge liquor treatment plant with nitrification. *Water Sci. Technol.* **63** (12), 2838–2845.
- Hao, X. D., Heijnen, J. J. & van Loosdrecht, M. C. M. 2002 Sensitivity analysis of a biofilm model describing a one-stage completely autotrophic nitrogen removal (CANON) process. *Biotechnol. Bioeng.* **77**, 266–277.
- Henze, M., Gujer, W., Mino, T. & van Loosdrecht, M. C. M. 2000 *Activated Sludge Models ASM1, ASM2, ASM2d and ASM3*. IWA Scientific and Technical Report No. 9, IWA Publishing, London, UK.
- Hiatt, W. C. & Grady Jr., C. P. L. 2008 An updated process model for carbon oxidation, nitrification and denitrification. *Water Environ. Res.* **80** (11), 2145–2156.
- Kampschreur, M. J., Temmink, H., Kleerebezem, R., Jetten, M. S. M. & van Loosdrecht, M. C. M. 2009 Nitrous oxide emission during wastewater treatment. *Water Res.* **43** (17), 4093–4103.
- Law, Y., Ni, B. J., Lant, P. & Yuan, Z. 2012 N₂O production rate of an enriched ammonia-oxidising bacteria culture exponentially correlates to its ammonia oxidation rate. *Water Res.* **46** (10), 3409–3419.
- Law, Y., Lant, P. & Yuan, Z. 2013 The confounding effect of nitrite on N₂O production by an enriched ammonia-oxidizing culture. *Environ. Sci. Technol.* **47** (13), 7186–7194.
- Mampaey, K. E., Beuckels, B., Kampschreur, M. J., Kleerebezem, R., van Loosdrecht, M. C. M. & Volcke, E. I. P. 2013 Modelling nitrous and nitric oxide emissions by autotrophic ammonia-oxidizing bacteria. *Environ. Technol.* **34** (12), 1555–1566.
- Ni, B. J., Yuan, Z., Chandran, K., Vanrolleghem, P. A. & Murthy, S. 2013 Evaluating four mathematical models for nitrous oxide production by autotrophic ammonia-oxidizing bacteria. *Biotechnol. Bioeng.* **110** (1), 153–163.
- Ni, B. J., Peng, L., Law, Y., Guo, J. & Yuan, Z. 2014 Modeling of nitrous oxide production by autotrophic ammonia-oxidizing bacteria with multiple production pathways. *Environ. Sci. Technol.* **48** (7), 3916–3924.
- Pan, Y., Ni, B. J., Lu, H., Chandran, K., Richardson, D. & Yuan, Z. 2014 Evaluating two concepts for the modelling of intermediates accumulation during biological denitrification in wastewater treatment. *Water Res.* **71**, 21–31.
- Stenström, F., Tjus, K. & la Cour Jansen, J. 2014 Oxygen-induced dynamics of nitrous oxide in water and off-gas during the treatment of digester supernatant. *Water Sci. Technol.* **69** (1), 84–91.
- Yang, J., Trela, J., Plaza, E. & Tjus, K. 2013 N₂O emissions from a one stage partial nitrification/anammox process in moving bed biofilm reactors. *Water Sci. Technol.* **68** (1), 144–152.
- Yu, R., Kampschreur, M. J., van Loosdrecht, M. C. M. & Chandran, K. 2010 Mechanisms and specific directionality of autotrophic nitrous oxide and nitric oxide generation during transient anoxia. *Environ. Sci. Technol.* **44** (4), 1313–1319.
- Zhou, Y., Pijuan, M., Zeng, R. J. & Yuan, Z. 2008 Free nitrous acid inhibition on nitrous oxide reduction by a denitrifying-enhanced biological phosphorus removal sludge. *Environ. Sci. Technol.* **42** (22), 8260–8265.

First received 12 March 2015; accepted in revised form 6 October 2015. Available online 27 October 2015